

DIFFERENTIABLE QUANTUM ARCHITECTURE SEARCH FOR JOB SHOP SCHEDULING PROBLEM

Yize Sun^{1,2} Jiarui Liu¹ Yunpu Ma^{1,2} Volker Tresp^{1,2}

¹Ludwig-Maximilians-University Munich ²Siemens AG
Munich, Germany

ABSTRACT

The Job shop scheduling problem (JSSP) plays a pivotal role in industrial applications, such as signal processing (SP) and steel manufacturing, involving sequencing machines and jobs to maximize scheduling efficiency. Before, JSSP was solved using manually defined circuits by variational quantum algorithm (VQA). Finding a good circuit architecture is task-specific and time-consuming. Differentiable quantum architecture search (DQAS) is a gradient-based framework that can automatically design circuits. However, DQAS is only tested on quantum approximate optimization algorithm (QAOA) and error mitigation tasks. Whether DQAS applies to JSSP based on a more flexible algorithm, such as variational quantum eigensolver (VQE), is still open for optimization problems. In this work, we redefine the operation pool and extend DQAS to a framework JSSP-DQAS by evaluating circuits to generate circuits for JSSP automatically. The experiments conclude that JSSP-DQAS can automatically find noise-resilient circuit architectures that perform much better than manually designed circuits. It helps to improve the efficiency of solving JSSP.

Index Terms— JSSP-DQAS, JSSP, QAS, SP

1. INTRODUCTION

Quantum computing (QC) and quantum machine learning have rapidly developed in many areas [1–8]. Different quantum algorithms have been applied to industrial fields, for example, SP [9, 10], image processing [11, 12], quantum architecture search (QAS) [13–17], optimization problem [18], and scheduling problems [18–20]. Due to the hardware noises, the performance of the quantum circuit can be reduced [14, 21]. Moreover, available qubits are limited, and cannot solve complex problems without a training process.

VQA is a leading hybrid quantum algorithm combining quantum and classical computation to solve complex problems [22]. In VQA, a quantum circuit with adjustable parameters is optimized using classical optimizers given a specific objective function. Combinatorial optimization problems aim to optimize an objective function within a large configuration space defined by discrete values while adhering to specific

constraints. VQA, such as VQE and QAOA, is suitable for solving combinatorial optimization problems.

JSSP is one of the combinatorial optimization problems and can be formalized as a quadratic unconstrained binary optimization (QUBO) problem. It abstracts the job shop as a model of a working location containing some available machines and a set of jobs. Each job includes a sequence of operations. JSSP has been solved by VQA using a predefined circuit architecture [18]. However, manually finding a task-specific, hardware-efficient, and noise-resilient quantum circuit is hard. We try to optimize the quantum circuit architecture for solving JSSP.

DQAS, as one of the QAS algorithms, is proposed in [14]. It is a gradient-based algorithm and aims to choose a sequence of unitaries to form a circuit that can optimize a task-specific objective function. DQAS relaxes the parameter determining the circuit structure into a continuous domain, allowing the gradient descent search. It performs excellently searching for noise-resilient circuits with error mitigation [13, 14]. Although QAOA has been successfully tested with DQAS [14], QAOA is often limited by circuit deep and architectures, which may restrict its performance. Since VQE views the circuit as an approximator of the ground state and can provide more flexibility, we consider using VQE for our framework JSSP-DQAS to search for a suitable circuit for JSSP.

In this work, we propose a new framework, JSSP-DQAS. It can design noise-resilient quantum circuit architectures efficiently and automatically. The searched circuits outperform manually designed circuits and reduce hardware costs with fewer gates by keeping quantum features. Moreover, a shallow circuit outperforms a complex circuit for a simple task.

2. METHOD

Algorithm 1 shows an overview of our framework JSSP-DQAS containing four steps. The initialization step defines an operation pool \mathcal{O} , a circuit with p placeholders, the shared architecture parameter α and trainable weights θ of the parameterized circuit, an objective function, and a target value. A batch of circuit architectures is sampled in the training process according to the probabilistic model P . Each architecture calculates the local MSE loss between the predicted

Algorithm 1 DQAS for JSSP

Step 1: Initialization:

Initialize circuit with p placeholders, operation pool \mathcal{O} , α , θ , objective function and target value.

Step 2: Super-circuit training:

while Architecture search **do**

 Sample a batch of circuit architectures.

 Calculate global loss \mathcal{L} via Eq: 7

 Update α_t and θ_t via gradients $\nabla \mathcal{L}_\alpha$ and $\nabla \mathcal{L}_\theta$

end while

Circuit parameter tuning

Step 3: Get circuits:

Take top-K architectures for JSSP evaluation

Step 4: Evaluation of architectures:

Take the best performing architecture or retrain

and target values as the objective function. Then, the global loss \mathcal{L} comes out based on all sampled architectures' local objective function L . They use the gradient-based optimizer Adam to update α , θ , and the probability in P of each operation candidate. The top K circuit architectures are determined after the architecture search procedure. The fine-tuning process starts, which only updates θ , if necessary. Finally, we get the top K circuit architectures and fine-tuned θ . We use these designed circuits to solve JSSP and search the circuits again if their performances are bad.

2.1. Circuit and parameters

The circuit includes encoding, parameterized and measurement blocks. The encoding block prepares states for the parameterized blocks. The parameterized block stacked with p placeholders can be seen as a composition of a sequence of unitaries:

$$U = \prod_{i=0}^p u_i(\theta_i) \quad , \quad (1)$$

where θ_i is the trainable parameters of the corresponding unitary in the sequence. When u_i is a gate with no parameters, θ_i can be ignored. This work defines operation candidates and placeholders differently than the original DQAS. Each placeholder u_i covers all qubits instead of one qubit and accepts one element from the operation pool containing the working range. This way, the number of parameters for each placeholder depends on the operation type and working range, and the search space can thus be reduced by controlling the working range of operation candidates. The circuit architecture is updated based on the probabilistic model $P(U, \alpha)$. Each u_i will be placed by operation candidate $o_i \in \mathcal{O}$.

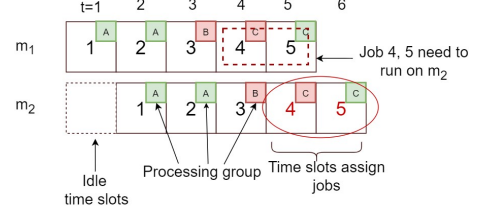


Fig. 1: The illustration of a JSSP task.

2.2. Operation pool

Operation pool \mathcal{O} in size of $s = |\mathcal{O}|$ is a set of quantum gate candidates. Each operation in \mathcal{O} contains the type of operation and its working range. If there is a circuit with five qubits, an operation pool can be defined with elements:

$$\mathcal{O} = \left\{ \underbrace{o_1}_{\text{Type}} : \underbrace{[0, 1, 2, 3, 4]}_{\text{Working range}}, o_2 : [0, 1], E : [0, 1, 2, 3, 4] \right\}. \quad (2)$$

The o_i denotes the type of operation, and it could be any 1-qubit gate or multi-qubit gate (e.g., RZ, U3, or CNOT). The corresponding array shows the range in which the operation works. For example, if operation $o_1 = \text{CNOT}$ is selected for one placeholder, five CNOT gates will work on all qubits with ring connections. This work defines two operation pools, op1 and op2. op1 contains candidates such as rz, rz both working on $\{[0, 1, 2, 3, 4], [0, 1, 2, 3], [1, 2, 3, 4]\}$, cz, cnot working on $[0, 1, 2, 3]$ and identity on all qubits. op2 contains almost the same candidates but has no cz.

2.3. Objectives and gradients

JSSP assigns J jobs to M machines at specific time slots [18]. Each job is assigned its due time and processing group. The processing time of each job is often identical. Each job needs to be processed on every machine, and the beginning time on the next machine cannot be earlier than the last. Each machine contains several idle time slots at the beginning or end. The total time slots of machine m is $T_m = J + i_m$, where J is the number of jobs and i_m is the number of idle time slots of machine m .

Fig. 1 illustrates a task of JSSP to be solved in this work, where time slots 1, 5 and 6 on machine 2 are idle, and jobs 4 and 5 need to be assigned on machine 2 in order. The red circle points out the optimal scheduler of this problem.

A solution of a JSSP consists of two schedules $x \in \mathbb{B}^{N_x}$ and $y \in \mathbb{B}^{N_y}$, where $\mathbb{B} = \{0, 1\}$, $N_x = \sum_{m=1}^M J(J + i_m)$ and $N_y = \sum_{m=1}^M i_m$. x represents real jobs and y represents dummy jobs that fill idle time slots. A value $x_{mjt} = 1$ represents that job j is assigned to machine m at time t . The value of a dummy job $y_{mt} = 1$ indicates that this dummy job is assigned to machine m at time t . The quadratic form

$Q : \mathbb{B}^{N_x} \times \mathbb{B}^{N_y} \rightarrow \mathbb{R}$ of JSSP is:

$$(x^*, y^*) = \underset{(x,y) \in \mathbb{B}^{N_x} \times \mathbb{B}^{N_y}}{\arg \min} Q(x, y) . \quad (3)$$

With cost and constraint penalties, the objective function Q becomes:

$$\begin{aligned} Q(x, y) = & c(x) + a_1 \sum_{m=1}^M \sum_{j=1}^J (g_{mj}(x) - 1)^2 \\ & + a_2 \sum_{m=1}^M \sum_{t=1}^{T_m} (l_{mt}(x, y) - 1)^2 \\ & + a_3 \sum_{m=1}^{M-1} \sum_{j=1}^J q_{mj}(x) + a_4 \sum_{m=2}^M \sum_{t=1}^{i_m-1} r_{mt}(y) , \end{aligned} \quad (4)$$

where $c(x)$ is the cost and the other terms correspond to constraints for 1. job assignment, 2. time assignment, 3. process order, and 4. idle slot. Details for each cost and constraint term can be found in [18]. a_1 - a_4 are coefficients used as weights to make a balance among constraints.

With quantum computing, finding the optimal solution to a QUBO problem is equivalent to finding the ground state of the Hamiltonian H created by replacing variables of $Q(x, y)$:

$$H = Q\left(\frac{I - Z_x}{2}, \frac{I - Z_y}{2}\right) , \quad (5)$$

where Z indicates PauliZ operators for binary vectors x, y .

We use CVaR to calculate the cost of JSSP. To make a simple notation, we use the concatenation of x, y , where $Q(z) = Q(x, y)$. We sample k bitstrings and calculate the energy $E_k(\theta)$ for each bitstring b_k , where $E_k(\theta) = Q(b_k(\theta))$. These energies are arranged in ascending order. This sample of energies $\{E_1(\theta), \dots, E_k(\theta)\}$ is put into the CVaR estimator to calculate the energy:

$$C(\theta) = \frac{1}{\lceil \alpha K \rceil} \sum_{k=0}^{\lceil \alpha K \rceil} E_k(\theta) . \quad (6)$$

The global objective function is defined as the total sum of local objectives according to the architecture distribution model $P(U, \alpha)$ and the energy of the bitstring of the optimal solution E_{target} :

$$\mathcal{L} = \sum_{U \sim P(U, \alpha)} L(U, \theta) , \quad (7)$$

where

$$L(U, \theta) = (C(\theta) - E_{\text{target}})^2 . \quad (8)$$

We will iteratively update the parameters by gradient descent, including the circuit parameter θ and the architecture parameter α . Since θ is independent of the architecture distribution, its gradient takes the form:

$$\nabla_{\theta} \mathcal{L} = \sum_{U \sim P(U, \alpha)} \nabla_{\theta} L(U, \theta) . \quad (9)$$

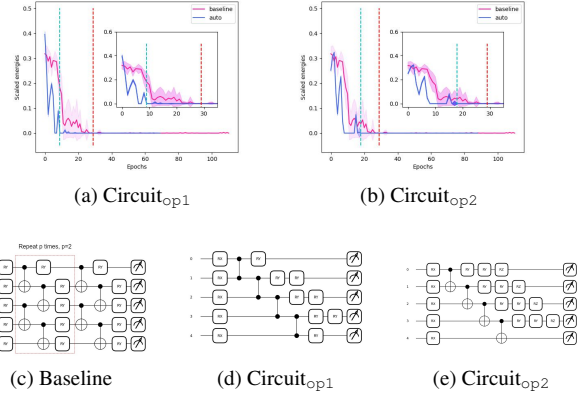


Fig. 2: Evaluation of newly found architectures on the simulator without noise. The results are averaged over 200 trials with the same initial parameters.

In practice, this gradient can be calculated by the parameter shift rules [23, 24]. The gradient of the architecture parameter matrix α is related to the architecture distribution and calculated as described in DQAS [14].

3. EXPERIMENTS AND RESULTS

3.1. Experiment setting

In this chapter, we conduct experiments with five qubits using JSSP-DQAS for the JSSP task described in Fig. 1 and defined in [18]. Their manually designed circuit, represented in Fig. 2c, is selected as our baseline. In the experiments, all qubits are initialized with the state $|0\rangle$ and applied rx gates with a rotation angle of π to form the encoding block. There is only one parameterized block containing four placeholders. For each learning step, we will update all placeholders.

The energies E are scaled to the range $[0, 1]$:

$$e = \frac{E - E_{\min}}{E_{\max} - E_{\min}} \in [0, 1] , \quad (10)$$

where E_{\min} and E_{\max} are the minimum and maximum energy. When $e \approx 0$, we reach the minimal energy and find the optimal solution.

3.2. Results and discussion

Fig. 2 shows the evaluation of newly found architectures on the simulator without noise. The automatically designed architectures converge faster than the baseline to the average solving point (ASP), which means the average results reach the optimal schedule within 20 epochs. The shadowed standard deviation areas of the learned circuits are much smaller than the baseline, indicating that circuits yield consistent outcomes for multiple trials, reflecting the learned architectures' stability, reliability and reproducibility.

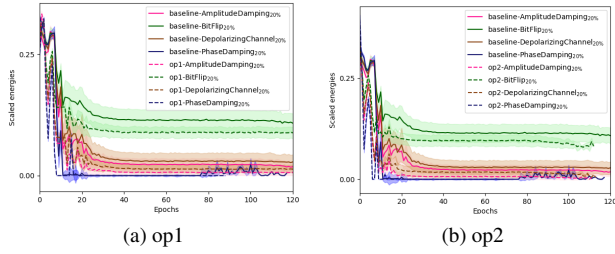


Fig. 3: Evaluation of newly found architectures on noisy simulator.

The best architecture $\text{Circuit}_{\text{op1}}$ derived from op1 in Fig. 2d begins with CZ gates. The type of controlled gates is different from that in the baseline. There are no redundantly parameterized blocks in $\text{Circuit}_{\text{op1}}$. $\text{Circuit}_{\text{op2}}$ derived from op2 in Fig. 2e has redundant gates on specific qubits, which might improve the training performance.

In general, more gates in a circuit, especially the controlled gates, indicate a higher building cost of the quantum circuit, while controlled gates provide quantum features by creating entanglements. $\text{Circuit}_{\text{op1}}$ and $\text{Circuit}_{\text{op2}}$ contain fewer gates than the baseline, while $\text{Circuit}_{\text{op1}}$ has the fewest. The searched circuits thus have lower building costs, keeping quantum features. Fewer parameterized gates and trainable parameters lead to a more straightforward quantum computation process. This simplification can improve the overall efficiency of the quantum circuit during training, resulting in faster convergence. Some noises and errors in a quantum circuit are caused by decoherence and gate imperfections. Using fewer gates can reduce the number of operations that cause noises or errors and lead to more reliable and stable circuits that converge faster.

In Fig. 3, we study the resistance of auto-generated circuits to noise. We form noise models by adding 20% noise of different types on each end of the qubit. The shadowed standard deviation areas of designed architectures are much smaller than the baseline, indicating those learned circuits yield consistent outcomes. Under BitFlip noise, the baseline and the searched circuit end with the average results much larger than the minimum energy. However, the ASP and the minimum energies found by designed circuits outperform the baseline in different models. Although because of the influence of noise, the learned circuits, including the baseline, do not find the accurate minimum energy in some trials, the automatically designed circuits are noise-resilient and more reliable in most cases.

In Fig. 4, we study the impact of placeholders and parameterized blocks during generating circuits. The red line indicates the number of gates and the ASP of the baseline is 23. The evaluation results show that as the number of placeholders and parameterized blocks increase, the number of gates in the generated circuits and the depth of the circuits increase

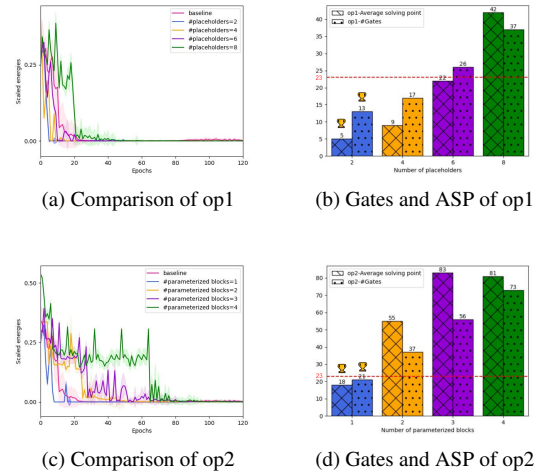


Fig. 4: (a) and (b) illustrate the impact of placeholders when generating circuits with op1. (c) and (d) illustrate the impact of parameterized blocks when generating circuits with op2.

and converge more slowly when solving a simple JSSP. The deeper the circuits are, the more parameterized gates need to be trained, resulting in more complex quantum calculations and slower convergence.

4. CONCLUSION AND OUTLOOK

In this work, we propose a framework JSSP-DQAS. The results show that it can design noise-resilient quantum circuit architectures efficiently and automatically. The searched circuits outperform the manually designed circuits. The newly discovered circuits with fewer gates reduce the hardware cost by keeping quantum features. Our experiments have demonstrated the beneficial impact of DQAS on scheduling problems. This work uses a shallow circuit and a large learning step for the training process. However, a better architecture might hide in a deep super-circuit in case of a complex task.

Acknowledgment

The project of this workshop paper is based on was supported with funds from the German Federal Ministry of Education and Research in the funding program Quantum Reinforcement Learning for industrial Applications (QLinda) and the Federal Ministry for Economic Affairs and Climate Action in the funding program Quantum-Classical Hybrid Optimization Algorithms for Logistics and Production Line Management (QCHALLENGE) - under project number 13N15644 and 01MQ22008B. The sole responsibility for the paper's contents lies with the authors.

5. REFERENCES

- [1] Jacob Biamonte, Peter Wittek, Nicola Pancotti, Patrick Rebentrost, Nathan Wiebe, and Seth Lloyd, “Quantum machine learning,” *Nature*, vol. 549, no. 7671, pp. 195–202, 2017.
- [2] Maria Schuld, Ilya Sinayskiy, and Francesco Petruccione, “An introduction to quantum machine learning,” *Contemporary Physics*, vol. 56, no. 2, pp. 172–185, 2015.
- [3] Raúl V Casana-Eslava, Paulo JG Lisboa, Sandra Ortega-Martorell, Ian H Jarman, and José D Martín-Guerrero, “Probabilistic quantum clustering,” *Knowledge-Based Systems*, vol. 194, pp. 105567, 2020.
- [4] Ji-An Li, Daoyi Dong, Zhengde Wei, Ying Liu, Yu Pan, Franco Nori, and Xiaochu Zhang, “Quantum reinforcement learning during human decision-making,” *Nature human behaviour*, vol. 4, no. 3, pp. 294–307, 2020.
- [5] SK Jeswal and S Chakraverty, “Recent developments and applications in quantum neural network: A review,” *Archives of Computational Methods in Engineering*, vol. 26, pp. 793–807, 2019.
- [6] Daoyi Dong, Chunlin Chen, Hanxiong Li, and Tzyh-Jong Tarn, “Quantum reinforcement learning,” *IEEE Transactions on Systems, Man, and Cybernetics, Part B (Cybernetics)*, vol. 38, no. 5, pp. 1207–1220, 2008.
- [7] Maria Schuld, Ilya Sinayskiy, and Francesco Petruccione, “The quest for a quantum neural network,” *Quantum Information Processing*, vol. 13, pp. 2567–2586, 2014.
- [8] Yunpu Ma, Volker Tresp, Liming Zhao, and Yuyi Wang, “Variational quantum circuit model for knowledge graph embedding,” *Advanced Quantum Technologies*, vol. 2, no. 7-8, pp. 1800078, 2019.
- [9] Yonina C Eldar and Alan V Oppenheim, “Quantum signal processing,” *IEEE Signal Processing Magazine*, vol. 19, no. 6, pp. 12–32, 2002.
- [10] Guang Hao Low and Isaac L Chuang, “Optimal hamiltonian simulation by quantum signal processing,” *Physical review letters*, vol. 118, no. 1, pp. 010501, 2017.
- [11] Fei Yan, Abdullah M Iliyasa, and Phuc Q Le, “Quantum image processing: a review of advances in its security technologies,” *International Journal of Quantum Information*, vol. 15, no. 03, pp. 1730001, 2017.
- [12] Zhaobin Wang, Minzhe Xu, and Yaonan Zhang, “Review of quantum image processing,” *Archives of Computational Methods in Engineering*, vol. 29, no. 2, pp. 737–761, 2022.
- [13] Yuxuan Du, Tao Huang, Shan You, Min-Hsiu Hsieh, and Dacheng Tao, “Quantum circuit architecture search for variational quantum algorithms,” *npj Quantum Information*, vol. 8, no. 1, pp. 62, 2022.
- [14] Shi-Xin Zhang, Chang-Yu Hsieh, Shengyu Zhang, and Hong Yao, “Differentiable quantum architecture search,” *Quantum Science and Technology*, vol. 7, no. 4, pp. 045023, 2022.
- [15] Thomas Fösel, Murphy Yuezhen Niu, Florian Marquardt, and Li Li, “Quantum circuit optimization with deep reinforcement learning,” *arXiv preprint arXiv:2103.07585*, 2021.
- [16] Li Ding and Lee Spector, “Evolutionary quantum architecture search for parametrized quantum circuits,” in *Proceedings of the Genetic and Evolutionary Computation Conference Companion*, 2022, pp. 2190–2195.
- [17] Shi-Xin Zhang, Chang-Yu Hsieh, Shengyu Zhang, and Hong Yao, “Neural predictor based quantum architecture search,” *Machine Learning: Science and Technology*, vol. 2, no. 4, pp. 045027, 2021.
- [18] David Amaro, Matthias Rosenkranz, Nathan Fitzpatrick, Koji Hirano, and Mattia Fiorentini, “A case study of variational quantum algorithms for a job shop scheduling problem,” *EPJ Quantum Technology*, vol. 9, no. 1, pp. 5, 2022.
- [19] Kazuki Ikeda, Yuma Nakamura, and Travis S Humble, “Application of quantum annealing to nurse scheduling problem,” *Scientific reports*, vol. 9, no. 1, pp. 12837, 2019.
- [20] Davide Venturelli, Dominic JJ Marchand, and Galo Rojo, “Quantum annealing implementation of job-shop scheduling,” *arXiv preprint arXiv:1506.08479*, 2015.
- [21] Poulami Das, Swamit Tannu, Siddharth Dangwal, and Moinuddin Qureshi, “Adapt: Mitigating idling errors in qubits via adaptive dynamical decoupling,” in *MICRO-54: 54th Annual IEEE/ACM International Symposium on Microarchitecture*, 2021, pp. 950–962.
- [22] Marco Cerezo, Andrew Arrasmith, Ryan Babbush, Simon C Benjamin, Suguru Endo, Keisuke Fujii, Jarrod R McClean, Kosuke Mitarai, Xiao Yuan, Lukasz Cincio, et al., “Variational quantum algorithms,” *Nature Reviews Physics*, vol. 3, no. 9, pp. 625–644, 2021.
- [23] Gavin E Crooks, “Gradients of parameterized quantum gates using the parameter-shift rule and gate decomposition,” *arXiv preprint arXiv:1905.13311*, 2019.
- [24] David Wierichs, Josh Izaac, Cody Wang, and Cedric Yen-Yu Lin, “General parameter-shift rules for quantum gradients,” *Quantum*, vol. 6, pp. 677, 2022.